What is behind all those lifetimes anyway? Where do we go from here?

Yi-Chun Chen[†], Bryan Q. Spring[‡], Chittanon Buranachai[‡], George Malachowski[#],

and Robert M. Clegg*[‡†]

[†]**Bioengineering Department**
University of Illinois at Urbana-Champaign, 1304 West Springfield Avenue, Urbana, IL 61801

[‡]**Center for Biophysics and Computational Biology**
University of Illinois at Urbana-Champaign, 607 South Mathews Avenue, Urbana IL 61801-3080

[#]**Bioscience Applications**, Pty. Ltd.
12 Scarborough Place, Melbourne 3031, Australia

***Department of Physics**
University of Illinois at Urbana-Champaign, Loomis Laboratory of Physics, 1110 West Green Street,
Urbana IL 61801-3080
Telephone: (217) 244-5620, Telefax: (217) 244-7187
E-mail: rclegg@uiuc.edu

ABSTRACT

Fluorescence lifetime-resolved imaging microscopy (FLIM) has made tremendous strides in the last two decades. Exciting applications are being presented weekly, an extensive diversity of instrumentation and commercial devices have appeared and have improved dramatically, sophisticated algorithms for analysis and interpretation are now available, and FLIM is being coupled to other imaging modalities, such as spectral dispersion and anisotropy. In other words, FLIM has matured considerably, and is approaching a point where it can be routinely applied by researchers who are not involved with the instrumentation and analysis side of things. The number of interested users in FLIM has almost certainly surpassed that of the audience that previously employed single channel fluorescence lifetime measurements (in a cuvette). The reason is, of course, the imaging capability of FLIM and its exciting possibilities for biological applications, especially FRET. In this lecture I will attempt to give an overview of where we have come from together with a personal judgment on where we stand, propose possible areas of growth that will be of importance for the future of FLIM, and discuss some specific challenges that remain, especially considering the unique nature of the FLIM measurement and the complex biological and medical systems that require innovative and novel solutions from the FLIM community.

Keyword list: FLIM, fluorescence lifetimes, frequency-domain, time-domain, imaging, wavelets, denoising, polar plot, morphology recognition, image analysis, model-free analysis

1. INTRODUCTION

The lifetime of a fluorophore in the excited state is simply the time that the molecule remains on the average in an electronically excited state after becoming excited by some mechanism. There are different mechanisms by which a molecule can become electronically excited: direct excitation by absorbing a photon, resonance energy transfer from another nearby excited molecule, intersystem crossing from an initial excited singlet state to a triplet state, and as a product of a chemical or biochemical reaction. In general, following the initial excitation to the excited state, the molecule will relax within picoseconds to the lowest singlet electronic state (called the S1 state) eventually attaining a thermodynamic Boltzmann distribution of its vibration manifold compatible with the S1 electronic potential. Often, although not always, the emission of a photon from the excited molecule takes place from this relaxed excited state. The

Multiphoton Microscopy in the Biomedical Sciences IX, edited by Ammasi Periasamy, Peter T. C. So,
Proc. of SPIE Vol. 7183, 718302 · © 2009 SPIE · CCC code: 1605-7422/09/$18 · doi: 10.1117/12.814952

electronic and molecular configurations, and the electronic energy level of the S1 state are sensitive to the immediate molecular environment of the excited molecule, and it is this sensitivity to the environment that makes fluorescence, especially the fluorescence lifetime, such a valuable probe of biological structures, cells and tissue.

There are many mechanisms by which the excited molecule in the S1 state can return to the ground state, one of which is by emitting a photon (fluorescence). Because the fluorescence competes kinetically with all the other pathways of de-excitation, the fluorescence lifetime, and the fluorescence intensity, report on the presence and the rates of the other pathways. The sensitivity and ease of measurement is the reason why fluorescence is extensively used to acquire information about the molecular processes that take place in the molecular neighborhood of the fluorescence probes. The fluorescence intensity is an indirect measure of the de-excitation process, because the intensity is the time integral of the dynamics. Since fluorescence is a dynamic process, it is best, and more informative, to record the dynamic relaxation directly. This is in a nutshell, the significance of measuring fluorescence lifetimes.

FLIM combines dynamic fluorescence lifetime measurements with fluorescence image acquisition. In the following we review the basic paradigm by which almost all lifetime-resolved fluorescence measurements can be interpreted in order to capture molecular mechanisms and identify molecular processes. The problems that arise when measuring and interpreting FLIM in complex biological samples will be discussed, as well as the effect of this complex environment on the accuracy and information content of the decay processes. We discuss some new aspects of image analysis and model-free FLIM analysis. Then a personal forecast will be made as to where FLI is headed, and the importance and need of new image analysis approaches.

2. THE BASIC MEASUREMENT AND THE FUNDAMENTAL FLUORESCENCE RESPONSE

Lifetime-resolved fluorescence imaging (FLI) measurements are carried out in several ways; however, the basic physics of the different measurements are essentially the same, differing in the instrumentation used to capture the lifetime decay. All techniques of FLI data acquisition are related to earlier methods of fluorescence lifetimes in cuvettes, which is a well developed and mature field of research, both from the point of view of data acquisition and analysis. Complications in FLIM arise from the sheer number of pixels that must be acquired separately in order to form a FLIM image with high spatial resolution. There are many reviews detailing the different technologies of FLIM data acquisition (many recent references can be found in [1, 2], and in two books to appear in 2009 [3, 4]. We will not discuss the defining features of these methods in detail, but see Sect. 3. However, the basic underlying method is identical in all cases. The sample is excited with a repetitive pulse of light (laser, lamp or LED). The measured temporal fluorescence response of the sample is described by the convolution of the actual form of the excitation pulse with the response of the fluorophore(s) to a delta function pulse: [5-9]:

$$F(t)_{meas} = \int_0^t E(t')\,F_\delta(t-t')\,dt' \tag{1}$$

$E(t')$ is the time dependence of the excitation event; this is usually a repetitive waveform, and can vary from a pure sinusoidal wave or a repetitive square wave to a repetitive series of pulses of short duration. $F_\delta(t-t')$ is the **fundamental fluorescence response** of the fluorescent sample to a single delta function excitation pulse, $E_\delta(t')$. t' is the time that $E_\delta(t')$ arrives to excite the sample, and $t-t'$ is the time, following t', that the measurement is made at time t. A delta function pulse is considered to be very short compared to any rate of fluorescence decay. The decay of every separate component of fluorescence (with singular lifetimes), excited directly by $E_\delta(t')$, can be described by the *fundamental fluorescence response, expressed as an exponential decay*.

$$F_\delta(t-t')_{meas} = F_\delta(t-t') = F_0 \exp(-(t-t')/\tau) \tag{2}$$

There may be many components that decay exponentially, either from the same chemical species in different environments, or from different chemical species. In heterogeneous environments of FLIM samples (e.g. biological cells) the heterogeneities of fluorescence lifetimes of even identical fluorescence species are usually more pronounced than in cuvette-type experiments, where the solvent and other buffer components are well defined and can be controlled by the experimenter. Assuming for the moment well defined individual multiple exponential decays (that is, with

singular lifetimes), *the fundamental fluorescence response is a sum of exponential decays*, each weighted with corresponding amplitudes and each with a different lifetime.

$$F_\delta\left(t-t'\right)_{meas} = \sum_i F_{\delta,i}\left(t-t'\right) = \sum_i F_{0,i}\exp(-(t-t')/\tau_i) \quad (3)$$

The inverse lifetimes, $1/\tau_i$, are the sum of all the rate constants of de-excitation of all the pathways leading out of the excited state of species. For non-interacting fluorophores each decay component contributes individually to the signal, and the measured signal is then described by Eq. 1, where $F_\delta\left(t-t'\right)_{meas}$ replaces $F_\delta\left(t-t'\right)$ in Eq. 1. It is also possible that there is essentially a continuous distribution of fluorescence lifetimes for one or more fluorescence species (caused by the heterogeneity of the molecular environment), and for each species with such a distribution that component of the sum is replaced by an integral over the distribution [2]. Distributions will be discussed further later.

When observing the fluorescence of the product of an excited state reaction, such as FRET, the excitation of the product of the excited state reaction is proportional to the decay function of the initially excited molecule that is reacting with the reactant form of the eventual product (e.g. the decay function of the "donor" $F_D(t)$ is the excitation function $E(t')$ of the "acceptor") and in that case Eq. 1 is the convolution of $F_D\left(t'\right)$ with $F_{A,\delta}\left(t-t'\right)$ of the acceptor. This will be important for some of the examples given below. Eq. 1 is a general way to describe the fluorescence response of a fluorophore, as long as we know the form of the excitation process.

3. THE "SO-CALLED" TIME- AND FREQUENCY-DOMAINS

It is traditional to refer to two main methods of FLIM experiments and analysis: the time-domain and the frequency-domain. In essence there is not a great distinction, and the reference is more historical than meaningful. As has been pointed out the two "domains" are related through their Fourier transforms. In general, in order to measure some kinetic process happening in a certain time range (for fluorescence, usually between picoseconds and nanoseconds) some part of the data acquisition must have the response and resolution of the same time range as the kinetics under study (for FLIM this is the time response of fluorescence). This is the same requirement in all kinetic experiments, and the initial detection of the fluorescence signal must have a high frequency band pass, or equivalently the primary detector must have a very fast time response. The excitation light must also be modulated with the time resolution (or frequency bandwidth) of the fluorescence decay one is interested in. This is true even if one is using random white noise to drive the excitation light and autocorrelation or power spectrum of the fluorescence signal to estimate the times; that is, the random noise must have the frequency bandwidth of the fluorescence dynamics [10]. In this manuscript we only point out some primary features of these acquisition methods. Although the same aspects pertain to single channel experiments, we are mainly interested in emphasizing points especially important for FLI measurements.

3.1 Time domain

The data acquisition is easy to picture in the time-domain – one just has to record the data directly at known times, and for defined periods, following the excitation pulses; if the excitation is sufficiently short, it is not necessary to deconvolute the excitation pulse from the recorded fluorescence time response in order to recover the fundamental fluorescence response; otherwise, the analysis must include such a deconvolution in the fitting process. Of course, if there is any process of the data acquisition instrumentation that is temporally convoluted with the primary fluorescence response before the final data acquisition, this must be deconvoluted, or at least taken into account in the fitting process. The data is then usually analyzed as a series of time decaying exponentials, often to determine the component amplitudes and relaxation times. Again, there are many ways of carrying out the analysis, and many of the methods are derived from earlier algorithm developments of single channel fluorescence lifetime measurements [11, 12]. If iterative fitting routines are used, this poses a major challenge with FLIM data. Whether scanning data acquisition or full field data acquisition (e.g. with CCD cameras [2] or quadrant detectors [13]) are used, the number of separate pixels to be analyzed can extend to 10^6 or more. This can take a relatively long time; different methods for carrying out such analyses have been reviewed [11, 14]

3.2 Frequency domain

In the frequency domain the initial signal detection is similar – the time progression of the fluorescence emission is detected with a detector that has the required time resolution. The frequency domain refers to the Fourier transform space of the temporal progression of the fluorescence response. The point in the data acquisition process where the data are best (or become) described in the frequency domain varies with the particular method of acquisition.

For instance, it is possible to simply take the Fourier transform of the repetitive time-domain signal (see the last paragraph) in order to transform the data from a time representation (after acquisition) to a frequency representation. This is not normally done; although, it was earlier a way to make initial guesses at the exponential parameters for later iterative fitting of single channel data. However, it may be advantageous to do this for a subsequent model independent analysis (see below). It is also possible to determine directly at the high frequency of the excitation modulation the phase delay and depth of modulation of each frequency component of the repetitive fluorescence signal relative to the excitation signal (or only the fundamental repetitive frequency) at the high frequency of excitation modulation. This is similar to a direct lock-in synchronous measurement of the signal; however, this is not advantageous, because the noise contribution at these high frequencies, due to the required bandwidth, is considerable. A common way of converting the signal to a frequency representation at lower frequencies is to modulate the initial time-resolved photodetected signal with the overall amplification factor of the detector at a frequency close to the frequency (10—400 MHz) of excitation modulation (heterodyne detection) or at the exact phase locked frequency of the excitation (homodyne detection). These two methods take advantage of synchronous detection, and reduce the bandwidth of the final detection to very low frequencies, reducing the noise, but retaining all the kinetic information of the signal components [15].

3.3 Which method to choose?

Even though we have emphasized that the basic premises of the data collection of all fluorescence lifetime measurements are similar, this does not mean that the instrumentation is similar, except for the fact that there must be a light source with some sort of repetitive modulation of the excitation light intensity, a way of focusing the light onto the sample (either by scanning a point or full field illumination), a detector capable of reacting to the dynamic fluorescence response, and a way to acquire the data into a computer for further analysis and display. There are definite advantages for each method of acquisition; some are exceptionally efficient in collecting and counting photons, some acquire data at exceptionally high rates, some have better temporal or spatial resolution, some can penetrate deeper into samples (e.g. tissue), and there are other minor as well as major differences and advantages. The prospective user has now an extended (and sometimes confusing) choice of different methods of FLIM data acquisition, and there are many firms that can now deliver just about every method of FLIM instrumentation that has been developed. In addition, FLIM measurements can be coupled with other microscopic methods, such as FCS, high resolution imaging, and single molecule detection. Of course, each different FLIM instrument has its own pros and cons, and exciting improvements in data acquisition equipment are constantly taking place. FLIM instrumentation has advanced from the phase of an interesting technology with possible future applications in a few laboratories, to a proven technique where the available instruments have high levels of performance and efficiency, high quality instruments are available commercially, and the FLIM technology is widely distributed in many laboratories as a workhorse experimental technique.

We mention only a few features of each data acquisition method; the reader is referred to the literature for detailed discussions.

3.3.1 Time domain

The time-domain has been implemented in two major optical configurations: scanning a focused laser beam (with two photon excitation, or using a single photon confocal arrangement) across the sample, or acquiring images in full field mode after exciting the full area of the sample at every position simultaneously. The scanning methods have become popular; especially after high performance commercial instruments have become available that can scan with point spread function spatial resolution, have picosecond time resolution, and under many circumstances can acquire high signal-to-noise photon counting quality data per pixel. The full field time-domain modes of acquisition usually only acquire a few time periods following excitation pulses, and the data analysis is not as sophisticated as the scanning modes; although, the data acquisition and analysis is usually much faster than the scanning modes. When trying to analyze fluorescence data in terms of a series of time decaying exponentials, it is critical to know accurately the temporal form $E(t')$, because the fundamental fluorescence response has been convoluted with the excitation pulse, and the fundamental fluorescence response must be deconvoluted from the actual time course of the acquired time recording of the fluorescence (this is not a problem if using repetitive very short excitation pulses, such as hundreds of femtoseconds of picoseconds (which are very short compared to the fluorescence decay times). Of course, in order to accurately attempt a multi-exponential fit to the data requires high counts are required at every pixel of interest. A consideration when performing time-domain data acquisition and analysis, especially when fitting each pixel with iterative algorithms, is the relative long time required from initiating the experiment until achieving a finished FLIM image. However, due to advances in the instrumentation and some new developments that accelerate the data analysis (including faster

computing power) this is becoming less acute, and for many experiments the time required to display a finished, analyzed FLIM image does not play a role. Also, as we will discuss below, it is not clear that it is always necessary, desired or even possible, to analyze data from complex biological samples and try to determine singular well defined lifetimes.

3.3.2 Frequency domain

For measurement and analysis of the time recording in the frequency domain, it is not necessary to know the form of the excitation pulse, because the frequency components of a Fourier decomposition of the signal are all separate from each other, and are analyzed separately, regardless of the form of the excitation pulse. The wave train of the excitation light can be repetitive delta function short pulses, sinusoidal forms, or any repetitive waveform. Because the excitation is a repetitive pulse train, it can be expressed as a Fourier series, and because each component of a Fourier series is orthogonal to all other components, each component of the fluorescence signal can be analyzed with digital Fourier techniques, which are non-iterative, easy to implement and very rapid. This advantage extends also to the acquisition process. The contributions of the different frequency components of the excitation pulse train can be determined either by measuring the modulation and phase contributions of the excitation, or by using a standard fluorophore of known phase and modulation behavior. It is not necessary to know the actual temporal waveform of the excitation pulse train. There is also often no reason to attempt to determine the actual underlying lifetimes. The behavior of the raw phases and modulations, which are easily and rapidly determined, are highly informative and often are quite sufficient, and sometimes preferred for following biological changes.

3.3.3 Common usage of the terms time- and frequency-domain

Even though, as we have indicated above, there is great overlap between the data acquisition and analysis of what is commonly referred to as the time-and frequency domains of FLIM (or of fluorescence lifetime-resolved measurements in general) we will use the terms “time-domain” and “frequency-domain” throughout the text wherever there is no major confusion. In general, the time-domain refers to an end analysis of the acquired signal according to a sum of exponential decays (Eq. 3), and analysis of the frequency-domain involves the analysis of the phase and level of demodulation of the signal. Of course the fluorescence temporal response is acquired in both cases.

4. SOME HISTORICAL COMMENTS ABOUT NON-IMAGING AND IMAGING LIFETIME INSTRUMENTATION AND MEASUREMENTS

It is interesting to review the history of non-imaging fluorescence lifetime measurements, and compare this to the development of FLIM. As usual, technological advances led the way to the first measurements of nanosecond lifetimes.

4.1 Phosphorescence lifetimes non-imaging and imaging

The spinning mechanical multi-slotted disk of Becquerel (a phosphoroscope) was the first instrument for measuring luminescence lifetimes; a sample could alternately be illuminated and the fluorescence observed by adjusting relative angular positions of the slits of two concentric synchronously rotating discs (with the sample between the two rotating discs) [16, 17]. In this original work, Becquerel was only able to determine lifetimes in the multiple microsecond time range (however, this was a major accomplishment). Through these types of experiments Becquerel discovered that many luminescent samples decayed much faster than could be captured with his simple instrumentation. Becquerel also developed the basic theoretical framework for the analysis that is discussed in section 2, and even discussed multiple lifetime components. Because of the long time of the delayed luminescence signal, the fast prompt fluorescence and scattering from the sample are completely suppressed, and an image of the long time emission could be observed. Therefore, this simple device could be considered as the first example of lifetime-resolved imaging. Many instruments for measuring non-imaging phosphorescence have been constructed, and it is still a very active field of research [18, 19].

Newton Harvey constructed the first imaging phosphorescence microscope [20]. 20-30 years later, microscopes capable of making lifetime-resolved phosphorescence imaging from biological material were further developed [21-25]. These microscopes were basically designed according to the Becquerel phosphoroscope. Using CCD image data acquisition, phosphorescence microscopes for determining phosphorescence decay times in an image appeared in the late 1980s and early 1990s [26-29]. Later delayed luminescence instruments (for lifetimes longer than microseconds) have been applied for measuring levels of oxygen in biological samples. Delayed luminescence microscopy (with lifetimes of hundreds of microseconds to milliseconds) has more recently been shown to be valuable for imaging the lifetime-

resolved luminescence of chelate-encapsulated lanthanides that are used as protein labels [30]. Prompt fluorescence is completely depressed. Delayed luminescence imaging is usually not considered under the label of FLIM, but it is still an active field of research.

4.2 Fluorescence lifetimes non-imaging

For measuring the nanosecond lifetimes, it was necessary to develop faster light shutters. In 1875 , the Kerr Effect was invented by John Kerr [31], and this provided a "light shutter" that could react into the nanosecond time region [32]. With this, Gaviola [33-35] and others were able to determine accurate lifetimes in the nanosecond time range. The subsequent improvements were mainly instrumentation developments, except for a few years when there was a question of the nature of the dwell time of a molecule in its excited state [36]. The early experiments did not have the convenience of very fast electronics, and therefore the major methods involved spatial time delays and pure optical apparatus. As electronic detectors entered the scene, the field of fluorescence lifetime determination took off in earnest [37, 38]. As soon as commercial photon counting instrumentation became available, many labs began fluorescence lifetime measurements. And because of the high accuracy possible with photon counting data, interest grew in developing fitting algorithms capable of differentiating closely lying lifetimes and distributions, with sophisticated error analysis. The same was later true of frequency domain experiments with multiple frequencies [39-43]. The point we want to make here, is that the initial major advances were related to the instrumentation, which was of course parallel to, and actually initiated by, technological developments. The major emphasis on the data analysis followed naturally after the instrumentation was capable of producing high quality data. The applications of the single channel lifetime measurements were mainly in fields like chemistry, physics, biophysics, and biochemistry, and usually involved separated and purified biological components of proteins, lipids and nucleic acids. There were relatively few (compared to the other fields of research) experiments done on larger scale biology samples (cells, tissue and whole mammalian and plant systems). After high quality single channel fluorescence lifetime instrumentation became available, the applications followed rapidly, and new specialized instruments were developed as spin-offs.

4.3 Fluorescence lifetime-resolved imaging

The major obstacle for applications of fluorescence lifetimes to biology was the difficulty of imaging the lifetime data. By the late 1980s confocal microscopy began to be developed in earnest, and rapidly became established and commercialized (it was invented in 1957 by Minsky, but was difficult to implement), and detectors with full field electronic image acquisition (CCDs, image intensifiers and diode arrays) were also available. But there was no convenient way to determine lifetime-resolved images with thousands to millions of image pixels. There were some initial early pioneering attempts by a few who realized the eventual use of nanosecond lifetime imaging in biological samples. These instruments basically used the available single channel instrumentation to measure lifetimes in biological samples imaged with available optical microscopes, but they did not really acquire images *per se*.

The first report of a fluorescence lifetime measurement (in the nanosecond time range) in optical microscopes was carried out in the frequency domain by Venette as early as 1959 [44]. Venette's instrument was developed at the same time as the frequency domain instrumentation of non-imaging fluorescence lifetime measurements [37, 38]. The intermediate image was focused through a small hole, which selected the spatial location within an image that one wanted to study. The light was modulated via a standing ultrasonic grating at 5-10 MHz. The excitation light and fluorescence were detected with separate photomultipliers (PM). The modulated fluorescence signal was phase detected using a homodyne technique (the reference and sample PM were modulated at the same frequency as the excitation light). The phase of the modulation on the reference PM was adjusted until the two signals were 180 degrees out of phase. By comparing the phase of the fluorescence signal relative to a scattering signal, the phase, and therefore the lifetime, of the emitted fluorescence could be estimated. The instrument was capable of dissecting the image into areas of interest, and can therefore be classified as an imaging fluorescence lifetime instrument. Lifetime measurements were carried out on fluorphores bound to the nuclei of tumor cells, as well as autofluorescence of biological tissue samples. Vanetta's instrument was far ahead of the general interest of the scientific community for measuring fluorescence lifetimes in microscopic samples, and was even developed before most of the phosphorescence microscopes.

It took almost 20 years before other fluorescence lifetime imaging measurements in microscopes were attempted. These measurements were carried out by comparing decay curves from an analog simulator with the fluorescence decay on an oscilloscope [45, 46], with a homemade digital averager [47-49], and by using Ortec photon counting instrumentation [50-52]. Because of low signal to noise, the measurement times were very long especially for photon counting methods when multi-exponential analyses were attempted. Just as for the single channel lifetime measurements,

the next phase of progress had to wait on advances in commercial electronics. The data acquisition electronics were either homemade, or not meant for weak signals from a microscope, compared to cuvette-based non imaging fluorescence lifetime measurements. The light sources were also not convenient lasers, but pulsed nitrogen lamp [52] or a nitrogen pumped tunable dye laser [47].

4.4 What took the time to implement FLIM?

The field of nanosecond fluorescence lifetime measurements (non-imaging) was well underway by the late 1970s, and commercial instrumentation (in both the time- and frequency domain) and highly sophisticated data analysis were available. The advantages and importance of incorporating lifetime-resolution in single channel fluorescence measurements was well appreciated by physicists, chemists and biochemists. However, the possibility of quantifying optical imaging measurements was only beginning to become available to most biology researchers involved in microscopy. Apparently, at the time, there was no motive for extending the lifetime measurements to images. This was to a great extent due to two factors: 1) the lack of suitable fast detectors and opto-electronic and computer data acquisition components and 2) probably because the biology research community did not appreciate the exciting possibilities for extending lifetime-resolved measurements to fluorescence images. The field of FLIM did not start in earnest until the late 1980s. This timing coincided with the ready availability of advanced charge coupled device cameras (CCDs), image intensifiers and scanning confocal microscopes, and fast data acquisition that could handle very large data sets. As is often the case, it is not easy to distinguish the desire of researchers in making certain experiments and the ability to do so that is often limited by readily available instrumentation. Therefore, it is not surprising that the "dawn of FLIM" took place in a few research laboratories with ready expertise in time-resolved fluorescence, fast electronics and usually a strong interest in biological problems; a review with references to many of the subsequent publications from many research groups is available [1]. However, immediately following the initial publications and announcements at international meetings, FLIM attracted the attention of many laboratories; and eventually industry became convinced of the utility and the market for FLIM.

4.5 Where are we now?

FLIM instrumentation has improved greatly in the last years. The instrumentation advances and increasing number of publications have led to a rapid expansion of FLIM applications, and a realization by the biology research community of the advantages and potential of FLIM for their biological studies. Most of these applications involve resolving the spatial locations of diverse rates of fluorescence response and forming a lifetime image. FLIM has great advantages for differentiating multiple fluorescence components, determining accurate concentrations, and is the best way to quantify FRET. While new ideas, improvements and implementations of FLIM emerge regularly from the university research labs and industry, the available FLIM instrumentation can be considered to be mature and reliable. FLIM can be said to have entered the application era, so much so that it is difficult to keep track of the publications. The topics of the talks and posters of this SPIE meeting attest to the rapid development of FLIM applications, as well as to the continual instrument improvement and new instrumentation designs. It is clear that lifetime resolved images can be acquired from any mode of fluorescence imaging, extending from single molecules, cells, tissue to whole body applications.

5. OK – WE CAN GATHER THE FLIM IMAGES; WHAT CAN THEY TELL US?

5.1 The pathways that compete with fluorescence for exiting the excited sate determine the lifetime.

The fluorescence lifetime reports on all the different pathways that a molecule can return to its ground state from an electronically excited state. The probability per unit time (rate) for a molecule to exit the excited state by the fluorescence pathway does not usually change; but the *measured* rate of fluorescence decay (inverse of the measured lifetime) is a sum of all the rate constants of all the available pathways of de-excitation. The common ways to exit an excited state, with their associated rate constants, are: fluorescence (k_f), non-radiative transitions (k_{nr}, heat and vibrational transfer), dynamic quenching (k_q, collisions with other molecules, such as ions), intersystem crossing (k_{isc}, from the initially excited singlet state to the triplet state), energy transfer (k_{et}, usually FRET), photodestruction (k_{ph}, by which the molecule is destroyed), and excited state chemical reaction (k_{ch} , sometimes changing the molecule, and sometimes not). Except the fluorescence pathway, each of these rates depends sensitively on the molecular environment of the fluorophore. The fluorescence quantum yield of a particular fluorophore is the ratio of the rate of exiting the excited state by emitting a photon to the sum of the rate constants of all pathways available to the excited molecule for exiting the excited state; or in other words, it is the ratio of the *measured* lifetime to the lifetime of the molecule if the

only pathway available were the fluorescence pathway. This simple relation is the basis of almost all quantitative fluorescence experiments.

Of course, the form of the measured time-dependent fluorescence response depends on the mode (the temporal form) of excitation according to the convolution in Eq. 1.

5.2 What is one traditionally trying to obtain from a fluorescence lifetime experiment?

The power of fluorescence is derived from the sensitivity of the average dwell time of a molecule in an electronically excited state to the immediate environment of the fluorophore. In general, fluorescence photons are messengers and fluorophores are spies. That is, we are not interested in investigating the fluorescence mechanism *per se*, rather we use fluorescence to inquire about properties regarding the sample. Fluorescence lifetime measurements have been extensively applied in single channel experiments and have been proven to show unique advantages in answering detailed molecular mechanistic questions. In cuvette-type, single-channel measurements, great emphasis has traditionally been placed on highly accurate data acquisition and associated sophisticated analysis to determine and distinguish individual lifetimes that represent detailed molecular mechanisms. The sample is usually completely under the control of the experimenter, and is therefore relatively uncontaminated. A great amount of work has been invested in first-round analysis of the data; for instance, fitting the fluorescence response to some model of exponential decays in order to determine individual well defined lifetimes and corresponding amplitudes. In FLIM experiments, there is a caveat to this type of analysis – the assumption is that the sample is uncontaminated and simple enough to expect that such an analysis clearly represents the underlying physical reality. In many cases the goal of a FLIM study with a complex, functional biological object is different than the single channel studies on relatively pure samples. If there are distributions of lifetimes, one can also try stretched exponentials [53]. In FLIM studies with living biological cells or tissue, common questions are: 1) where is a particular biological component located in a cell, 2) how close are two molecules to each other (FRET), 3) what is the index of refraction or polarity of some specific location in a cell compared to another location, 4) what is the pH or the concentration of some ion such as Calcium at particular locations, 5) can we follow the conformational change of a component of a cell or the binding of a ligand to a protein, 6) etc.? Fluorescence lifetime measurements in cuvettes have provided an efficient and exceptional opportunity to quantify more precisely the underlying physical molecular and biological processes influencing fluorescence measurements, and similar expectations should be expected of FLIM. To achieve this end, enormous progress has taken place on the instrumentation side, and highly sophisticated FLIM instruments are available that can deliver reproducible and precision data (and hardware improvements are continuing), and reliable commercial instruments have recently become available. In FLIM, the challenge is now to combine the quantifying features of fluorescence lifetime-resolved measurements with the revealing, but more qualitative, visualization features of spatially resolved imaging that are so vital for understanding biological systems.

5.3 What is different for FLIM analysis?

In general, the major objective of data analysis of FLIM data has usually remained similar to the traditional methods used in single channel experiments. That is, the goal of direct time-domain data acquisition is to separate individual exponential components using lifetime-resolution, and determine as accurately as possible lifetime values and their corresponding pre-exponential factors (this involves the deconvolution of the "true" fluorescence from the excitation waveform and instrument factors). The latter is also true of the frequency domain, where the phase and modulation data are often analyzed to determine corresponding underlying exponential decay parameters. This is natural, because the fundamental fluorescence response of a single component is an exponential decay, and one is, after all, supposed to be measuring fluorescence lifetimes. However, perhaps a better term would be "lifetime-resolved fluorescence". The suggestion here is not just a semantic attempt to change the terminology. It is known from much earlier work that very high accuracy is required to carry out a successful detailed multi-component analysis, and usually FLIM data does not have the required signal-to-noise ratio. Even if the signal-to-noise is respectable, it is very difficult to decide how many underlying exponentially decaying components contribute to a measured signal [11, 54], and major errors in interpretation lurk under such numerical analyses. In cuvette-type experiments, where the signal-to-noise level is much higher than in FLIM and the sample is reasonably "uncontaminated" with extraneous fluorescence, one can often alleviate some problems by changing the experimental conditions, such as the temperature, solvent composition, concentrations, etc.. Such an opportunity does not usually present itself in FLIM experiments in biological cells and tissue. This is the motivation behind our title "What is behind all those lifetimes anyway". Even if the raw signal-to-noise ratio is sufficient to attempt such a detailed analysis, the fluorescence from a complex biological sample is not expected to be truly represented by well-defined individual components, or even a simple single distribution of lifetimes

from a single component [55]; at least if it were the case, that would be exceptional. Fluorophores are sensitive to their immediate environment, and the environment of biological samples is highly heterogeneous. And there are usually contributions to the fluorescence from indigenous fluorophores. This is simultaneously the advantage and the demise presented to the FLIM user.

5.4 Taking advantage of extra information to assist the analysis of FLIM data

Because of the difficulties discussed in the last section, methods have been developed to assist in the data analysis. There are several common hardware techniques to help identify selected fluorescence components, and distinguish multiple component contributions, which should make a FLIM analysis more reliable and less ambiguous. For instance, new stable, selective fluorophores that emit far to the red are being developed to avoid as much as possible the contributions of the indigenous fluorphores. Some of these compounds, including the fluorescence proteins, are useful for FLIM. Special filters for different fluorophores are also available for targeting as much as possible the fluorescence response to a specific molecule. Spectral FLIM, where the lifetime-resolved signal is acquired over the fluorescence spectrum, is becoming more widespread, and this, coupled with FLIM, can be a major assistance in identifying different components or different populations of certain components, for instance, when analyzing a FRET signal (see Becker et al. [56] and Rueck et al. [57] and references therein). We discuss this below in conjunction with the polar plot. Global analysis [58-61] has also proven valuable in FLIM, and has been applied extensively previously in single channel fluorescence lifetime determinations [62-65]. Both global and spectral analysis methods have been successfully applied for some time to data from chemical kinetic experiments, such as rapid mixing and relaxation kinetics; the data in these cases represent the progress of a chemical reaction.

5.5 FLIM combines lifetime-resolution with spatial resolution. How to unite them?

Because FLIM is applied more frequently for investigating elaborate biological structures at different levels of complexity, it is natural to inquire 1) how best to extract maximal information from the FLIM images, 2) how to analyze and interpret specifically targeted FLIM data arising from complex biological samples that are significantly obscured by contributions from background and interfering fluorescence, and 3) how to employ well known image analysis techniques to merge the spatial, morphological image information with the lifetime-resolved signals. These questions are especially important now that such powerful instrumentation is available. And the FLIM technique is not limited to microscopes, and there are applications using normal macroscopic camera imaging as well as endoscopes, and these applications amplify the analysis problems.

A major challenge for FLIM is to analyze the data and present the results of the analysis to the user so that the major revealing features of the sample relevant to the particular biological experiment can easily be recognized. The usual and straight forward way is to present images of “lifetimes” in color coding, often accompanied by bump mapping the intensity with the lifetime parameters on the same display. The particular analysis depends of course on the particular questions being asked; however, the usual lifetime-resolved parameters derived are still “lifetimes”, and as discussed above, the lifetimes may be hard to define and relate to single components. On the other hand, the added spatial feature of FLIM presents new opportunities for analysis. Just as for normal optical imaging (non-lifetime-resolved), image analysis methods can help recognize information that is not obvious by just looking at the FLIM image. This is the topic of the rest of the manuscript.

6. NON-ITERATIVE DATA REGRESSION (CHEBYSHEV POLYNOMIALS)

FLIM images consist of thousands to millions of pixels, and if one analyzes the data with a numerical iterative fit at every pixel (such as fitting a series of exponentials to time-domain FLIM), the analysis time can be very long. Fourier analysis is exceptionally time efficient for analysis of data in the frequency domain because it is non-iterative (only one pass through the data is required). Are there analogous algorithms available so one can analyze data as a series of exponentials directly? Yes. We have developed a non-iterative transform method that is rapid, accurate, and avoids false minima. The method has been presented in detail in previous publications [66, 67]; here we only summarize the method and indicate the advantages. Examples can be found in the above references. Such algorithms can save extraordinary amounts of time.

The idea is to characterize a discrete function by a series of discrete orthogonal Chebyshev polynomials. The Chebyshev polynomial transform [68] produces coefficients of the continuous Chebyshev polynomials of the first kind, which are specific for the particular function being fitted (similar to the coefficients of a Fourier series). These polynomials have particular advantages for our case, and are described in many textbooks regarding orthogonal

polynomials in general [69]. The problem is then reduced to solving an algebraic equation, instead of fitting with an iterative method. This improves the speed of analysis by orders of magnitude.

An application is shown in a recent paper [67] where the Chebyshev technique was used to account for an exponentially decaying signal due to photolysis of homodyne frequency domain FLIM data. Originally such photolysis artifacts were handeled by interative fitting algorithms. In this case, the recorded fluorescence is a sinusoidal signal decaying over the time of data acquisition. The improvement in the speed of fitting the FLIM data when using Chebyshev polynomials compared to an interative method to account for the exponential decay of the FLIM signal is dramatic. The error analysis is comparable to iterative fitting [67]. This method is applicable to a large number of functions representing the fluorescence response.

7. POLAR PLOTS – MODEL FREE FLIM ANALYSIS

The analysis of the frequency-domain data, whether initially acquired as a frequency dependent signal or by Fourier transforming the data (either during data acquisition or later digitally), involves the measured phase and demodulation factor of the fluorescence response relative to the repetitive excitation wave form. The polar plot [70-75] (also referred to as a "phasor plot" [76] , an "A/B plot" [77, 78], or as a plot of the Fourier Transform pairs [79]) is a way to display the frequency characteristics (modulation fraction and phase) of signals that are described in the time-domain by exponential decays (where the pre-exponential factors can be positive or negative). Polar plots and similar frequency domain characterizations of data (e.g. Cole-Cole plots) have been used extensively to analyze and display dielectric dispersion data [80-83] and calculate the frequency characteristics of electronic circuits [84]. It is applicable to all physical systems that are excited with repetitive perturbations.

The fundamental frequency component of the fluorescence response that is composed of N separate independent underlying fluorescence components can be expressed as [8]

$$F(t)_{meas} = \left[\sum_i F_{0,i}\tau_i + \sum_i \frac{F_{0,i}\tau_i}{1+j\omega\tau_i} e^{j\omega t} \right] = \left[\sum_i F_{0,i}\tau_i + e^{j\omega t} \sum_i \frac{F_{0,i}\tau_i}{\sqrt{1+(\omega\tau_i)^2}} e^{-j\tan^{-1}\omega\tau_i} \right]. \quad (4)$$

$1 \le i \le N$. In real terms this is,

$$\left[F(t)_{meas} \right]_{real} = \left[\sum_i F_{0,i}\tau_i + \sum_i F_{0,i}\tau_i M_{\omega,i} \cos\left(\omega t - \phi_{\omega,i}\right) \right]. \quad (5)$$

The first sum, $\sum_i F_{0,i}\tau_i$, is the time independent (steady-state intensity) signal, $F_{meas,ss}$. The modulation and phase of the ith component are $M_{\omega,i} = 1/\sqrt{1+(\omega\tau_i)^2}$ and $\phi_{i,\omega} = \tan^{-1}\omega\tau_i$. The fractional contribution of species *i* to the measured steady state intensity is

$$\left[\text{fractional steady-state intensity of species i}\right] \equiv \alpha_i = F_{0,i}\tau_i / \sum_i F_{0,i}\tau_i \,;\; \sum_i \alpha_i = 1 \quad , \quad (6)$$

If the signal is normalized to the average steady state intensity, the normalized signal in complex notation is

$$\frac{F(t)_{meas}}{F_{meas,ss}} = 1 + \sum_i \frac{\alpha_i}{1+j\omega\tau_i} e^{j\omega t} = 1 + e^{j\omega t} \sum_i \alpha_i M_i \left[\cos\left(\phi_{i,\omega}\right) + j\sin\left(\phi_{i,\omega}\right) \right] \quad (7)$$

The terms $1/(1+j\omega t)$ and $M_i\left[\cos\left(\phi_{i,\omega}\right) + j\sin\left(\phi_{i,\omega}\right)\right]$ can be represented in a polar plot, which is a Cartesian x-y plot where $x = M_i \cos\left(\phi_{i,\omega}\right)$ and $y = M_i \sin\left(\phi_{i,\omega}\right)$ (see Eq. 7). If there is a single exponential component, all points lie on a semicircle (where $0 \le x \le 1$, and $0 \le y \le 0.5$) for any particular values of ω or τ . It turns out that for situations common for FLIM experiments it is convenient, diagnostic and informative to express (and analyze) the data in terms of polar plot, even for multiple times, and also for cases involving excited state reactions, such as acceptor fluorescence of FRET. Examples are given below after explaining the use of wavelets and denoising in regard to FLIM. The polar plot is a model-free depiction of the data, because the modulation and phase are directly determined, with no model. Also the way we carry out the experiment, there is no iterative fitting – digital Fourier techniques are used instead (which are equivalent); so the analysis is very rapid.

8. WAVELETS, DENOISING AND ALL THAT

8.1 What is a wavelet transform?

Wavelet transforms extract features within an image by selective filtering of localized space/scale characteristics of images using a multi-scale analysis scheme. It is a way to detect spatial frequency characteristics of image data at a local scale. On the other hand, two-dimensional Fourier image analysis reports on spatial frequencies in an image on a global scale. The Fourier transform of an image is a function of frequency only and produces a power spectrum of the frequency components on a global scale, but does not keep a record of the spatial locations of the frequency components. Windowed Fourier transforms analyze fixed localized regions of signals or images, but produce edge effects [85]. Also, the wavelet transform has a continuous "window" size over the full spatial frequency spectrum. However, in practice, digital wavelet transforms with are sufficient for many applications.

The wavelet multi-resolution decomposes a signal into its spatial or temporal frequency components. Wavelets are generalized local basis functions that can be stretched (dilated) and translated in both space and frequency. Wavelet transformations have units of both space and frequency (scale). Stretched wavelet basis functions correlate with spatial resolution of low frequency scale components – coarse features; and, contracted wavelet basis functions correlate with high spatial frequencies and fine structure. The dilation/contraction property sets the spatial extent, and the translation property locates the position within the image. Thus, the wavelet transform produces a matrix of coefficients at *each* pixel for *each* space/scale frequency. The wavelet coefficient matrix is obtained by translating the wavelet across the image, for various degrees of wavelet dilation/stretching, in the horizontal, vertical and diagonal directions. Thereby, the spatial orientation of objects can also be discerned with wavelets.

There are two sets of localized functions: 1) a scaling function and 2) an associated wavelet function. The scaling function is equivalent to a low-pass filter, and the wavelet is comparable with a band-pass filter [86]. The image is passed through a series of "filter banks" of dilated wavelets together with the associated scaling functions [87]. Morphologies are selected in the image with successively narrower spatial frequency band-pass (higher detail) and lower spatial resolution (less detail). The original image is decomposed into multi-resolution "approximation" (lower frequencies) and "detail" (higher frequency) coefficient matrices. The approximation is the low-frequency filtered image and the detail has the high-frequency components, for a particular scale. The low pass approximation image at some iteration of the wavelet procedure has been filtered of high frequencies. No data are lost; the original image can be recreated exactly by applying the inverse wavelet transform. Two low pass scaled images can be subtracted to select morphologies in the image with spatial frequencies in the differential bandpass region. The inverse transform with the coefficients in this band pass spatial frequency creates an image with morphologies corresponding to the selected localized spatial frequencies. The band passed image can then be used for the FLIM analysis.

Wavelets have only recently been used in fluorescence imaging [88]. There are many different wavelet transforming functions [89]. In imaging, wavelets are most often used for denoising [90-92], image compression [88, 93-95], location of dominant effects in an image [96], edge detection [97], and for object detection before particle tracking [98]. Wavelets have not been applied to FLIM measurements until recently.

8.2 Wavelets applied to homodyne frequency-domain FLIM

Frequency-domain, homodyne instruments have been previously described [2, 7, 8].

We have found wavelet and denoising techniques to be valuable to enhance the analysis of video-rate homodyne FLIM images: 1) Wavelet transforms are useful for selecting objects according to their spatial morphology (see also Pelet et al. [61]); and to separate fluorescence lifetime components originating from different spatial morphologies. Both the fluorescence intensity and fluorescence lifetimes of unwanted background components can be removed from the data using wavelet based filtering of spatial morphologies. 2) We have adopted an advanced image analysis technique to remove select types of noise from homodyne FLIM, which was originally designed exclusively for removing photon noise from intensity images. We have reported the efficacy of the wavelet transforms, which can automatically select localized morphologies in images based on their spatial frequencies, for analyzing FLIM images [74]. Often one knows the approximate morphology in cells one is interested in, and these regions in images can be recognized from their local morphologies, which transform into particular spatial frequency band pass regions. Regions with different spatial frequency characteristics can be removed, even when they overlap spatially with the regions of interest. We use a homodyne, frequency domain FLIM data acquisition; the wavelet transform is applied to each of the

phase selected fluorescence intensity images before the FLIM data is analyzed to extract the phase and modulation values. The background intensity (that is often a diffuse low spatial frequency contribution) can be effectively removed, as well the contribution of the background lifetime component to the lifetime [74]. In addition, contributions to the fluorescence (and therefore to the phase and modulation) from objects in the image with different morphologically correlated spatial frequency band passes than the region of interest, can be identified and removed of the wavelet procedure.

8.3 Denoising applied to homodyne frequency-domain FLIM

The major sources of noise are the Poisson noise of the initial photo detection and the detector/data acquisition noise. In our instrument, most of the detector noise is due to the variability in each of the photoelectron multiplication steps in the microchannel plates (MCP) of the image intensifier. We have analyzed the total noise contributions following the photon gain through the electron multiplication process, through to the phosphor screen, onto the CCD and including readout noise. The two major contributions are due to the Poisson photon noise and the amplification factor of the MCP. We have used the treatment of interdependent noise propagation for cascading ICCD detectors, discussed by Frenkel et al. [99]. Theoretical considerations demonstrate that the final noise distribution for the homodyne FLIM system is a signal-dependent Gaussian distribution. Nowak and Willet developed algorithms (termed translational-invariant Haar denoising: TI-Haar) for removal of signal-independent noise following a normal distribution with a variance of unity [100]. Hence, in order to apply TI-Haar to homodyne FLIM data we carry out a variance stabilizing transform (VST) [101], which transforms the image into signal-independent noise with a variance of unity. Following denoising, the inverse VST is applied to the data to return the image to its familiar signal level. The VST is carried out based on empirical data collected with our FLIM instrument – a signal-noise curve carried out for the exact same instrument settings as the data to be denoised. Thus, the denoising routine is carried out using the TI-Haar in "Gaussian mode", rather than "Poisson mode"; we refer to this final noise removal process at "TI-Haar + VST".

9. EXAMPLES OF MODEL FREE ANALYSIS AND MORPHOLOGY RECOGNITION AND DENOISING

A homodyne FLIM data was simulated to demonstrate wavelet analysis and TI-Haar denoising. The modulation and demodulation frequency was set at 100 MHz. The fluorescence intensity image of the simulation is shown in Fig. 1(a). The background has a 0.5 ns lifetime with Gaussian intensity distribution in addition to a white readout noise. On top of the background, there are two larger ellipses with 3 ns lifetime and ten smaller ellipses with 2 ns lifetime. Inside of the larger ellipses, there are round objects and each has a lifetime of 1 ns. Poisson noise was added to the simulation data. Fig.1(b) is the polar plot analysis of every pixel from Fig. 1(a), which shows visually that there are four different distributions of lifetime pools. Except for the lifetime pool corresponding to the background only area, all of the other three pools have more than one lifetime component. Fig. 1(c) and Fig. 1(e) are the fluorescence intensity images of Fig. 1(a) after performing wavelet multi-resolution analysis. The wavelet scale chosen is determined by the spatial frequency of interest of the objects in the original image. Fig. 1(c) is the third-scale detail image, which highlights the edges of objects and produces only the intensity difference at the edges. Therefore, analyzing all the pixels onto Fig. 1(d) gives directly the lifetimes value of the three separate components. Note here that no prior model assumption is held during the wavelet and polar plot analysis. Fig. 1(e) is the fluorescence intensity image after subtracting the first two scales of detail and the 10^{th}-scale approximation image. In other words, the high-frequency noise and the low-frequency background are eliminated from the data, and the polar plot representation in Fig. 1(f) shows that the three lifetime pools have no background effect and more compact distribution due to noise removal. The gray scale bar of the image indicates the fluorescence intensity (in arbitrary units) and the gray scale bar for the polar plot represents the number of pixels with that value.

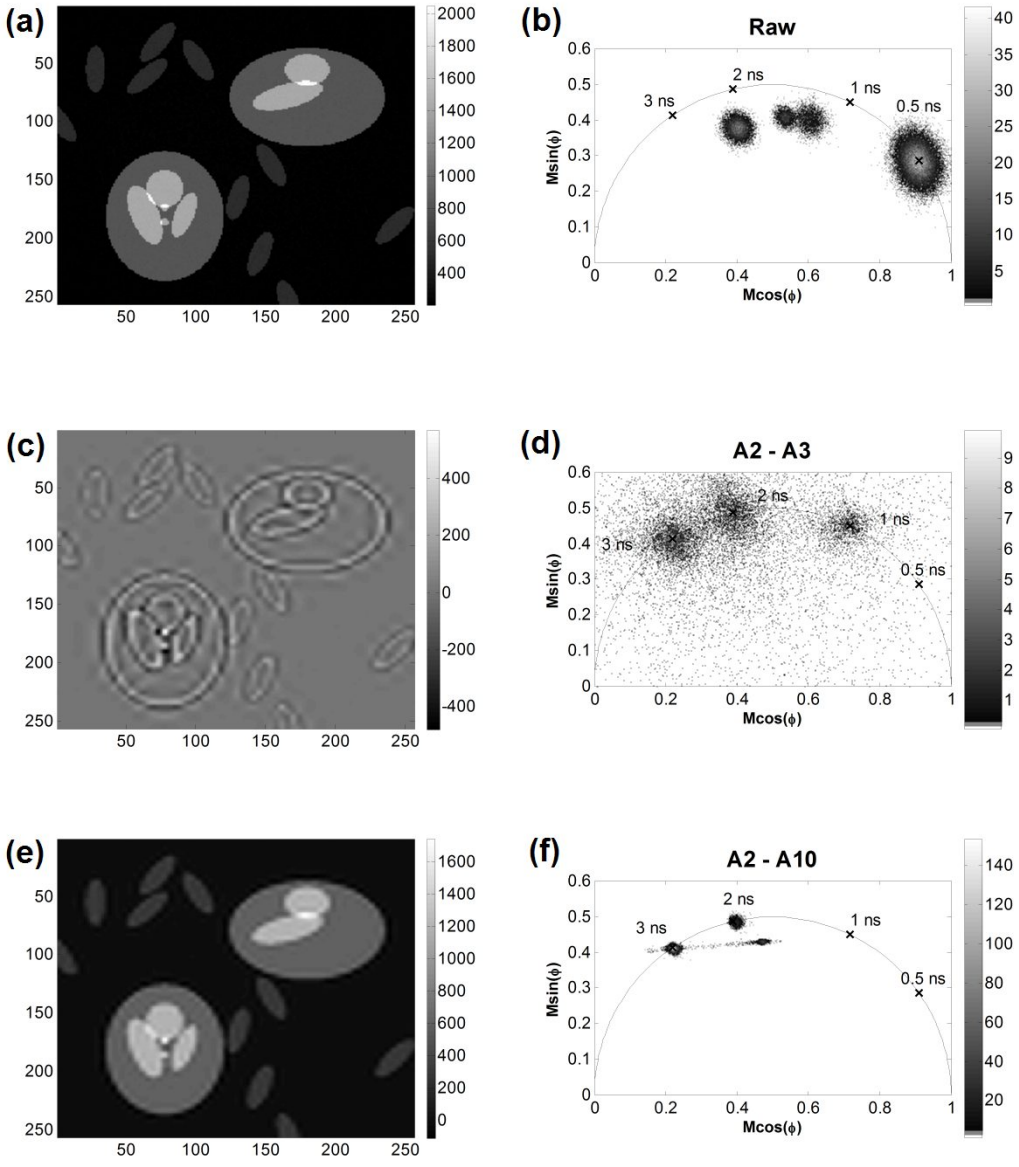

Figure 1. Wavelet analysis and the corresponding polar plot representation. 1(a): Fluorescence intensity of the simulated FLIM data; 1(b): polar plot analysis of all the pixels in 1(a); 1(c):fluorescence intensity at the third-scale wavelet detail of 1(a), which detects the edges of all the objects; 1(d) polar plot representation of 1(c) gives the exact lifetime values of the objects; 1(e):fluorescence intensity image after subtracting the two highest scales of detail and the 10^{th}-scale of approximation image; and 1(f):the polar plot of 1(e) shows the result after noise and background removal. The gray scale bar of the image indicates the fluorescent intensity (A.U.) and the one for the polar plot gives the value of pixel number.

Figure 2 emphasizes the power of wavelets in morphology recognition. All the 12 objects were recognized at the spatial frequency range of Fig. 1(e) (as shown in Fig. 2(a)). As an example, object number 6, 8, and 12 are selected for polar plot analysis in Fig. 2(b).

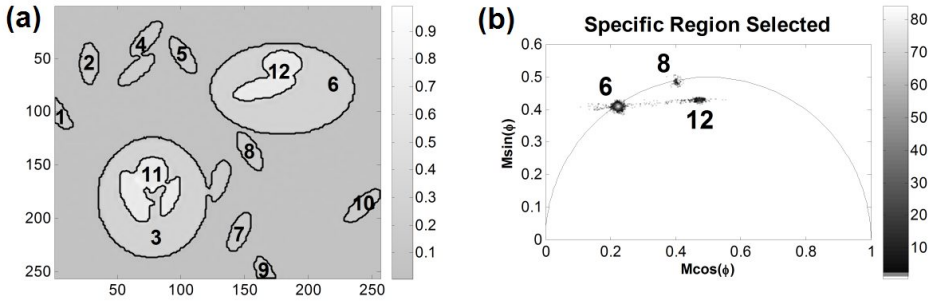

Figure 2. Morphology recognition at the spatial frequency range of Fig. 1(e). 2(a) demonstrates that all the 12 objects were recognized at this spatial frequency, and 2(b) is the polar plot analysis of the objects selected, which are 6, 8, and 12 in this case.

In Fig. 3 we used TI-Haar algorithm to remove the Poisson noise from the raw image. Compared with Fig. 1(b), the polar plot of the image after denoising (Fig. 3) has data points at almost a single value. With proper choice of denoising algorithm, one can apply wavelet analysis after denoising for better results (data not shown).

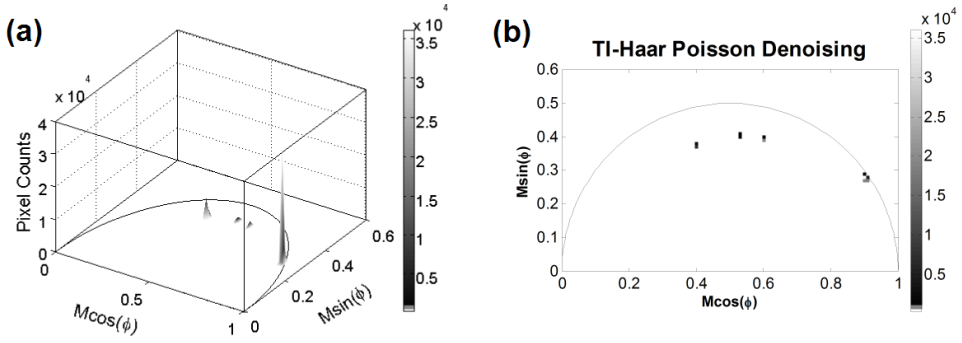

Figure 3. TI-Haar Poisson denoising of the original image. The polar plots in 3D (Fig. 3(a)) and 2D (Fig. 3(b)) show that data points falls onto almost a single point, on which they should be. Again, the gray scale bar indicates the pixel numbers. Notice the difference of this value between Fig. 1(b) and Fig. 3.

The homodyne FLIM measurement of fluorescent protein mCyPet inside of Chinese hamster ovary (CHO) cells are shown in Figure 4. The sample was measured in phosphate buffered saline and at 40 MHz. Fig. 4(a) is the fluorescence intensity image of the cells, and the polar plot analysis of the raw data is in Fig. 4(b). After applying "TI-Haar + VST" denoising process, the polar plot results are in Fig. 4(c) and Fig. 4(d). Two lifetime distributions are revealed clearly, and the smaller peak is not clearly seen in Fig. 4(b) because of the noise.

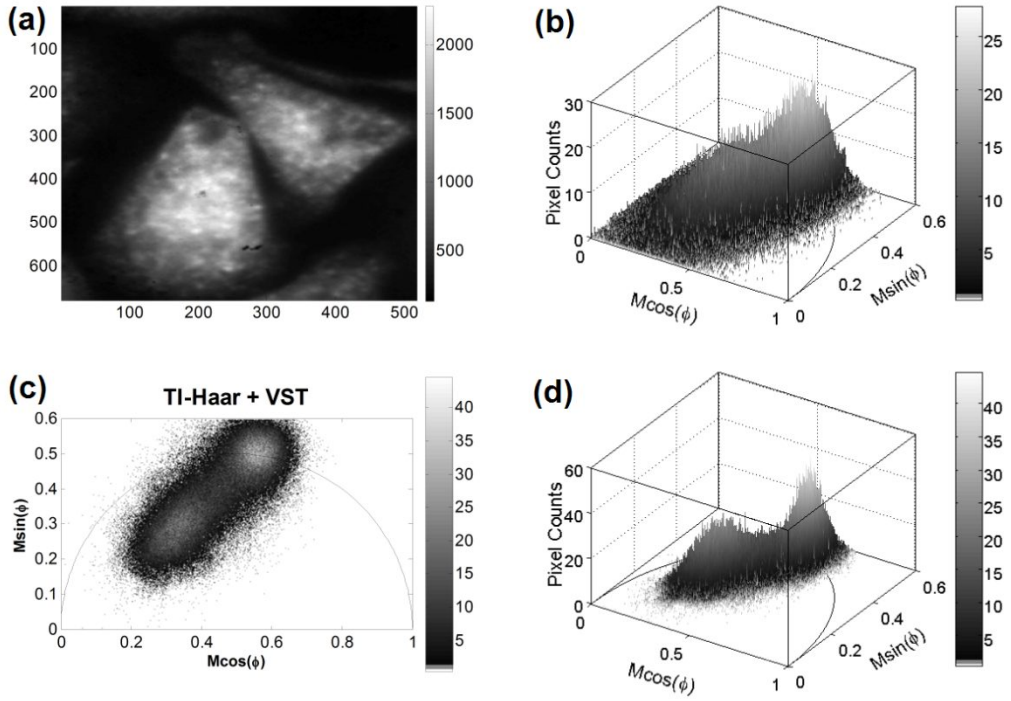

Figure 4. FLIM measurement of mCyPet before and after "TI-Haar + VST" denoising (100x objective). 4(a): Fluorescence intensity image of mCyPet in CHO cells; 4(b): Polar plot analysis of the raw image; 4(c) and 4(d): Polar plot of denoised data shown in 2D and 3D respectively.

10. REFERENCES

[1] van Munster, E.B. and Gadella, T.W.J., [Fluorescence Lifetime Imaging Microscopy (FLIM)], in *Adv Biochem Engin/Biotechnol*, Springer-Verlag, Berlin, 143-175, (2005).

[2] Redford, G.I. and Clegg, R.M., [Real-Time Fluorescence Lifetime Imaging and FRET using Fast Gated Image Intensifiers], in *Molecular Imaging: FRET Microscopy and Spectroscopy*, A. Periasamy and Day, R.N., Editors, Oxford University Press, New York, 193-226, (2005).

[3] Periasamy, A. and Clegg, R.M., eds. [FLIM Microscopy in Biology and Medicine], Boca Raton: Taylor & Francis, Boca Raton, (2009).

[4] Gadella, T.W.J., ed. [FRET and FLIM Techniques], Elsevier Inc., Laboratory Techniques in Biochemistry and Molecular Biology, Vol. 33 560 (2009).

[5] Birks, J.B., [Photophysics of Aromatic Molecules], Wiley, London. 704, (1970).

[6] Schneider, P.C. and Clegg, R.M., "Rapid acquisition, analysis, and display of fluorescence lifetime-resolved images for real-time applications," Review of Scientific Instruments 68(11), 4107-4119 (1997).

[7] Clegg, R.M., Schneider, P.C., and Jovin, T.M., [Fluorescence Lifetime-Resolved Imaging Microscopy], in *Biomedical Optical Instrumentation and Laser-Assisted Biotechnology*, A.M. Verga Scheggi, et al., Editors, Kluwer Academic Publishers, Dordrecht, Boston, London, 143-156, (1996).

[8] Clegg, R.M. and Schneider, P.C., [Fluorescence Lifetime-Resolved Imaging Microscopy: A General Description of the Lifetime-Resolved Imaging Measurements], in *Fluorescence Microscopy and Fluorescent Probes*, J. Slavik, Editor, Plenum Press, New York, 15-33, (1996).

[9] Dern, H. and Walsh, J.B., [Analysis of Complex Waveforms], in *Physical Techniques in Biological Research: Electrophysiological Methods, Part B*, W.L. Nastuk, Editor, Academic Press, New York, 99-218, (1963).

[10] Chandler, D.E., Majumdar, Z.K., Heiss, G.J., and Clegg, R.M., "Ruby Crystal for Demonstrating Time- and Frequency-Domain Methods of Fluorescence Lifetime Measurements," J Fluoresc 16(6), 793-807 (2006).

[11] Cundall, R.B. and Dale, R.E., eds. [Time-resolved fluorescence spectroscopy in biochemistry and biology], Plenum, New York, NATO ASI series. Series A, Life sciences, ed. F. NATO Advanced Study Institute on Time-Resolved Fluorescence Spectroscopy in Biochemistry and Biology (1980 : Saint Andrews, Vol. 69 785 (1983).
[12] Eaton, D.F., "Recommended methods for fluorescence decay analysis," Pure & Appl. Chem. 62(8), 1631-1648 (1990).
[13] Emiliani, V., Sanvitto, D., Tramier, M., Piolot, T., Petrasek, Z., Kemnitz, K., Durieux, C., and Coppey-Moisan, M., "**Low-intensity two-dimensional imaging of fluorescence lifetimes in living cells**," Applied Physics Letters 83(12), (2003).
[14] Becker, W., ed. [Advanced Time-Correlated Single Photon Counting Techniques], Springer, New York, Springer Series in Chemical Physics, Vol. 81 359 (2005).
[15] Goldman, S.J., [Frequency Analysis, Modulation and Noise], Dover, New York. 434, (1948).
[16] Becquerel, E., [La Lumiere. Ses Causes et Ses Effets], Paris. Librairie de Firmin Didot Freres. 377, (1868).
[17] Becquerel, E., "Memoire sur l'analyse de la lumière émise par les composés d'uranium phosphorescents.," Ann. de chim. et phys. 27, 539 (1871).
[18] Winefordner, J.D., "**Time-resolved phosphorimetry**," *Acc. Chem. Res.* 2 (12), 361-367 (**1969**).
[19] Strambini, G., Balestreri, E., Galli, A., and Gonnelli, M., "Effects of Sugars and Polyols on the Stability of Azurin in Ice. ," J Phys Chem B 112(14), 4372-4380 (2008).
[20] Harvey, E.N. and Chase, A.M., "The phosphorescence microscope.," Rev. Sci. Instr. 13, 365-368 (1942).
[21] Vialli, M., "Indirizzi di ricerca nel campo della istoluminescenza.," Z. wiss. Mikrosk. 66, 164-170 (1964).
[22] Polyakov, Y.S., Rosanov, Y.M., and Brumberg, E.M., "The setting installation for studying the phosphorescence of microobjects.," Cytologie SSSR. 8, 677-681 (1966).
[23] Zotikov, A.A., "Some possibilities of the phosphorescence microscopy for the study of cells and chromatin," Acta Histochem.(suppl) 26, 215-217 (1982).
[24] Zotikov, A.A. and Polyakov, Y.S., "Investigation of the phosphorescence of cells of various types with the phosphorescence microscope.," Izvestiya Akademii Nauk. SSSR Seriya. Bio. Esckaya. 2, 277-280 (1975).
[25] Zotikov, A.A. and Polyakov, Y.S., "The use of the phosphorescence microscope for the study of the phosphorescence of various cells.," Microscop. Acta. 79, 415-418 (1977).
[26] Jovin, T.M., Arndt-Jovin, D.J., Marriott, G., Clegg, R.M., Robert-Nicoud, M., and Schormann, T., [Distance, wavelength and time: the versatile 3rd dimensions in light emission microscopy.], in *Optical Microscopy for Biology.*, B. Herman and K. Jacobson, Editor, Wiley-Liss, New York, 575-602, (1990).
[27] Jovin, T.M., G. Marriott, G., Clegg, R.M., and Arndt-Jovin, D.J., "Photophysical processes exploited in digital imaging microscopy: fluorescence resonance energy transfer and delayed luminescence.," Ber. Bunsenges. Phys. Chem. 93, 387-391 (1989).
[28] Beverloo, H.B., van Schadewijk, A., van Gelderen-Bode, S., and Tanke, H.J., "Inorganic phosphors as **new** luminescent labels for immunocytochemistry and time-resolved microscopy.," Cytometry **1**(**1**), **784-792** (**1990**).
[29] Marriott, G., Clegg, R.M., Arndt-Jovin, D.J.a., and Jovin, T.M., "Time resolved imaging microscopy: Phosphorescence and delayed fluorescence imaging," Biophys. J. 60 1374-1387 (1991).
[30] Vereb, G., Jares-Erijman, E.A., Selvin, P.R., and Jovin, T.M., "Temporally and spectrally resolved imaging microscopy of lanthanide chelates.," Biophysical Journal 74, 2210-2222 (1998).
[31] Kerr, J., Phil. Mag. 1, 337 (1875).
[32] Abraham, A. and Lemoine, T., Comp. Rend. Acad. Sci 129, 206 (1899).
[33] Gaviola, E., "Die Abklingzeiten der Fluoreszenz von Farbstofflösungen," Z. Physik 35, 748-756 (1926).
[34] Gaviola, E., "**Das Abklingungszeiten der Fluoreszenz von Farbstoffloesungn**," Ann. d. Physik 81, 681-710 (1926).
[35] Gaviola, E., "Ein Fluorometer. Apparat zur Messung von Fluoreszenzabklingungszeiten.," Z. Physik 42, 853-861 (1927).
[36] Gaviola, E., "On time lags in fluorescence and in the Kerr and Faraday effects.," Physical Review 33, 1023-1034 (1929).
[37] Birks, J.B. and Dawson, D.J., "Phase and modulation fluorometer," J. Sci. Instr. 38, 282-295 (1961).
[38] Birks, J.B. and Little, W.A., "Photo-Fluorescence Decay Times of Organic Phosphors," Proceedings of the Physical Society Section A 66(10), 921-928 (1953).
[39] Gratton, E., Jameson, D.M., and Hall, R., "Multifrequency phase and modulation fluorometry," Ann. Rev. Biophys. Bioeng. 13, 105- 124 (1984).
[40] Gratton, E. and Limkeman, M., "A continuously variable frequency cross-correlation phase fluorometer with picosecond resolution," Biophysical Journal 44(3), 315-24 (1983).
[41] Gratton, E., Limkerman, M., Lakowicz, J.R., Maliwal, B.P., Cherek, H., and Laczko, G., "Resolution of mixtures of fluorophores using variable-frequency phase and modulation data.," Biophys. J. 46, 479-486 (1984).
[42] Valeur, B., [Molecular Fluorescence: Principles and Applications], Wiley-VCH, Weinheim. 387, (2002).
[43] Lakowicz, J.R., [Principles of Fluorescence Spectroscopy], Kluwer Academic/Plenum Publishers, New York, 2nd ed., (1999).
[44] Venetta, B.D., "Microscope Phase Fluorometer for Determining the Fluorescence Lifetimes of Fluorochromes," Rev. Sci. Instrum. 6(6), 450-457 (1959).
[45] Loeser, C.N. and Clarck, E., "Intrecellular fluorescence decay time of aminonaphthalene sulfonate," Experimental Cell Research 72, 485-488 (1972).

[46] Loeser, C.N., Clarck, E., Maher, M., and Tarkmeel, H., "Measurement of fluorescence decay time in living cells," Experimental Cell Research 72, 480-484 (1972).
[47] Bottiroli, G., Prenna, G., Andreoni, A., Sacchi, C.A., and Svelto, O., "Fluorescence of Complexes of quinacrine mustard with DNA. I. Influence of the DNA base composition on the decay in bacteria.," (1979).
[48] Andreoni, **A.**, Sacchi, C.A., S. Cova, S., Bottiroli, G., and Prenna, G., in ***Lasers in Physical Chemistry and Biophysics***, J. Joussot-Dubien, Editor, Elsevier Scientific, Amsterdam, 413-424, (1975).
[49] Andreoni, **A.**, Sacchi, C.A., Svelto, O., Longoni, A., Bottiroli, G., and Prenna, G., in ***Proceedings of the Third European Elecrro-Optics Conference***, H.A. Elion, Editor, SPIE, Washington, 258-270, (1976).
[50] Fernandez, S.M. and Berlin, R.D., "Cell surface distribution of lectin receptors determined by resonance energy transfer.," Nature ***264***, **411-415** (1976).
[51] **Herman, B.A.** and **Fernandez, S.M.**, "Changes in Membrane Dynamics Associated with Myogenic Cell Fusion," **J. Cell. Physiol.** 94, **253-264** (1978).
[52] Arndt-Jovin, D.J., Latt, S.A., Striker, G., and Jovin, T.M., "Fluorescence decay analysis in solution and in a microscope of DNA and chromosomes stained with Quinicrine.," The Journal of Histochemistry and Cytochemistry 27, 87-95 (1979).
[53] Benny Lee, K.C., Siegel, J., Webb, S.E.D., Le´veˆque-Fort, S., Cole, M.J., Jones, R., Dowling, K., Lever, M.J., and French, P.M.W., "**Application of the Stretched Exponential Function to Fluorescence Lifetime Imaging**," **Biophysical Journal** 81, 1265-1274 (2001).
[54] Istratova, A.A. and Vyvenko, O.F., "Exponential analysis in physical phenomena," Review of Scientific Instruments 70(2), 1233-1257 (1999).
[55] Kremers, G.J., van Munster, E.B., Goedhart, J., and Gadella, J.T.W.J., "Quantitative Lifetime Unmixing of Multiexponentially Decaying Fluorophores Using Single-Frequency Fluorescence Lifetime Imaging Microscopy," Biophys. J. 95, 378-389 (2008).
[56] Becker, W., Bergmann, A., and Biskup, C., "Multispectral Fluorescence Lifetime Imaging by TCSPC," Microscopy Research and Technique 70, 403-409 (2007).
[57] Rueck, A., Huelshoff, C., Kinzler, I., Becker, W., and Steiner, R., "SLIM: A New Method for Molecular Imaging," Microscopy Research and Technique 70, 485-492 (2007).
[58] Verveer, P.J. and Bastiaens, P.I.H., "Evaluation of global analysis algorithms for single frequency fluorescence lifetime imaging microscopy data," J Microsc 209(1), 1-7 (2003).
[59] Verveer, P.J., Squire, A., and Bastiaens, P.I., "Global analysis of fluorescence lifetime imaging microscopy data.," Biophys J. 78(4), 2127-37 (2000).
[60] Verveer, P.J., Squire, A., and Bastiaens, P.I., "Improved spatial discrimination of protein reaction states in cells by global analysis and deconvolution of fluorescence lifetime imaging microscopy data.," J Microsc. 202, 451-6 (2001).
[61] Pelet, S., Previte, M.J.R., Laiho, L.H., and So, P.T.C., "A Fast Global Fitting Algorithm for Fluorescence Lifetime Imaging Microscopy Based on Image Segmentation," Biophysical Journal 87 2807-2817 (2004).
[62] Knutson, J.R., Beechem, J.M., and Brand, L., "Simultaneous Analysis of Multiple Fluorescence Decay Curves: A Global Approach," Chemical Physics Letters 102(9), 501-507 (1983).
[63] Beechem, J.M. and Haas, E., "Simultaneous determination of intramolecular distance distributions and conformational dynamics by global analysis of energy transfer measurements," Biophys J 55(6), 1225-36. (1989).
[64] Vermunicht, G., Boens, N., and de Schryver, F.C., "Global analysis of the time-resolved fluorescence of alpha-chymotrypsinogen A and alpha-chymotrypsin powders as a function of hydration," Photochem Photobiol 53(1), 57-63. (1991).
[65] Krishna, M.M. and Periasamy, N., "Spectrally constrained global analysis of fluorescence decays in biomembrane systems," Anal Biochem 253(1), 1-7. (1997).
[66] Malachowski, G. and Ashcroft, R. *The Chebyshev transformation linearises the fitting of exponential, gaussian and binding function data.* in *Proceedings of the Australian Society of Biophysics, 10 Annual Meeting*. 1986. Canberra, Australia.
[67] Malachowski, G.C., Clegg, R.M., and Redford, G.I., "Analytic solutions to modelling exponential and harmonic functions using Chebyshev polynomials: fitting frequency-domain lifetime images with photobleaching," Journal of Microscopy 228(3), 282–295 (2007).
[68] **Boyd, J.P.**, [Chebyshev and Fourier Spectral Methods], DOVER Publications, Inc., 2nd ed., 590, (2000).
[69] Abramovitz, M. and Stegun, I.A., [Handbook of Mathematical Functions], Dover Publications, New York. 1046, (1972).
[70] Redford, G.I. and Clegg, R.M., "Polar Plot Representation for Frequency-Domain Analysis of Fluorescence Lifetimes," Journal of Fluorescence 15(5), 805-815 (2005).
[71] Redford, G.I., Majumdar, Z.K., Sutin, J.D.B., and Clegg, R.M., "Properties of Microfluidic Turbulent Mixing Revealed by Fluorescence Lifetime Imaging," Journal of Chemical Physics Accepted, (2005).
[72] Holub, O., Seufferheld, M.J., Gohlke, C., Govindjee, Heiss, G.J., and Clegg, R.M., "Fluorescence lifetime imaging microscopy of Chlamydomonas reinhardtii: non-photochemical quenching mutants and the effect of photosynthetic inhibitors on the slow chlorophyll fluorescence transients," Journal of Microscopy 226(2), 90-120 (2007).
[73] Buranachai, C. and Clegg, R.M., [Fluorescence Lifetime Imaging in Living Cells], in *Fluorescent Proteins: Methods and Applications.*, J. Rothnagel, Editor, Humana Press, (2007 in Press).

[74] Buranachai, C., Kamiyama, D., Chiba, A., Williams, B.D., and Clegg, R.M., "Rapid Frequency-Domain FLIM Spinning Disk Confocal Microscope: Lifetime Resolution, Image Improvement and Wavelet Analysis," Journal of Fluorescence Epub ahead of print, http://www.ncbi.nlm.nih.gov/pubmed/18324453 (2008).
[75] Colyer, R.A., Lee, C., and Gratton, E., "A Novel Fluorescence Lifetime Imaging System That Optimizes Photon Efficiency," Microscopy Research and Technique 71, 201–213 (2008).
[76] Digman, M.A., Caiolfa, V.R., Zamai, M., and Gratton, E., "The Phasor Approach to Fluorescence Lifetime Imaging Analysis," Biophysical Journal: Biophysical Letters 107, L14-L16 (2007).
[77] Clayton, A.H.A., Hanley, Q.S., and Verveer, P.J., "Graphical representation and multicomponent analysis of single-frequency fluorescence lifetime imaging microscopy data," J Microsc 213(1), 1-5 (2004).
[78] Hanley, Q.S. and Clayton, A.H.A., "AB-plot assisted determination of fluorophore mixtures in a fluorescence lifetime microscope using spectra or quenchers," Journal of Microscopy 218, 62-67 (2005).
[79] Berberan-Samtos, M.N., "The time dependence of rate coefficients and fluorescence anisotropy for non-delta production," Journal of Luminescence 50, 83-87 (1991).
[80] von Hippel, A.R., [Dielectrics and Waves], Wiley, New York. Vol. xii. (1954).
[81] Cole, K.S. and Cole, R.H., "Dispersion and Absorption in Dielectrics," J. Chem. Phys. 9, 341 (1941).
[82] Hill, N.E., Vaughan, W.E., Price, A.H., and Davies, M., [Dielectric Properties and Molecular Behavior], van Nostrand Reinhold Company, New York. (1969).
[83] Jonscher, A.K., [Dielectric relaxation in solids], Chelsea Dielectrics Press, London. (1983).
[84] Millman, J. and Halkias, C.C., [Integrated Electronics: Analog and Digital Circuits and Systems], McGraw-Hill Book Company, New York. 911, (1972).
[85] Walker, J., "Fourier Analysis and Wavelet Analysis," Notices of the AMS 44(6), 658-670 (1997).
[86] Mallat, S., "A theory for multiresolution signal decomposition: the wavelet representation," IEEE Transactions on Pattern Analysis and Machine Intelligence 11(7), 674-693 (1989).
[87] Hong, L., "Multiresolutional filtering using wavelet transform," Aerospace and Electronic Systems, IEEE Transactions on 29(4), 1244-1251 (1993).
[88] Bernas, T., Asem, E., Roinson, J., and Rajwa, B., "Compression of fluorescence microscopy images based on the signal-to-noise estimation," Microscopy Research and Technique 69(1), 1 (2006).
[89] Starck, J., Murtagh, F., and Bijaoui, A., [Image Processing and Data Analysis: The Multiscale Approach], Cambridge University Press. (1998).
[90] Starck, J.L. and Bijaoui, A., "Filtering and deconvolution by the wavelet transform.," Signal Processing 35, 195–211 (1994).
[91] Nowak, R. and Baraniuk, R., "Wavelet-domain filtering for photon imaging systems," IEEE Transactions on Image Processing 8(5), 666-678 (1999).
[92] Boutet de Monvel, J., Le Calvez, S., and Ulfendahl, M., "Image Restoration for Confocal Microscopy: Improving the Limits of Deconvolution, with Application to the Visualization of the Mammalian Hearing Organ," Biophysical Journal 80, 2455–2470 (2001).
[93] Shapiro, J., Center, D., and Princeton, N., "Embedded image coding using zerotrees of wavelet coefficients," Signal Processing, IEEE Transactions on [see also Acoustics, Speech, and Signal Processing, IEEE Transactions on] 41(12), 3445-3462 (1993).
[94] Grgic, S., Grgic, M., and Zovko-Cihlar, B., "Performance analysis of image compression using wavelets," Industrial Electronics, IEEE Transactions on 48(3), 682-695 (2001).
[95] Shapiro, J.M., "Embedded Image Coding Using Zerotrees of Wavelet Coefficients," IEEE Transactions on Signal Processing 41(I2), 3445-3462 (1991).
[96] Olivo-Marin, J.-C., "Extraction of spots in biological images using multiscale products," Pattern Recognition 35(9), 1989-1996 (2002).
[97] Willett, R. and Nowak, R., "Platelets: a multiscale approach for recovering edges and surfaces in photon-limited medical imaging," Medical Imaging, IEEE Transactions on 22(3), 332-350 (2003).
[98] Genovesio, A., Liedl, T., Emiliani, V., Parak, W., Coppey-Moisan, M., and Olivo-Marin, J., "Multiple particle tracking in 3-D+ t microscopy: method and application to the tracking of endocytosed quantum dots," Image Processing, IEEE Transactions on 15(5), 1062-1070 (2006).
[99] Frenkel, A., Sartor, M., and Wlodawski, M., "Photon-noise-limited operation of intensified CCD cameras," Applied Optics 36(22), 5288-5297 (1997).
[100] Willett, R. and Nowak, R., "Fast multiresolution photon-limited image reconstruction," Biomedical Imaging: Macro to Nano, 2004. IEEE International Symposium on, 1192-1195 (2004).
[101] Prucnal, P. and Saleh, B., "Transformation of image-signal-dependent noise into image-signal-independent noise," Opt. Lett 6, 316–318 (1981).